Strongly renormalized quasiparticles in UPt_3

Ikuto Kawasaki,[1,*] Kazuharu Takeuchi,[2] Shin-ichi Fujimori,[1] Yukiharu Takeda,[1] Hiroshi Yamagami,[1,3] Etsuji Yamamoto,[4] and Yoshinori Haga[4]

[1]*Materials Sciences Research Center, Japan Atomic Energy Agency, Sayo, Hyogo 679-5148, Japan*
[2]*Graduate School of Science, University of Hyogo, Kamigori, Hyogo 678-1297, Japan*
[3]*Department of Physics, Faculty of Science, Kyoto Sangyo University, Kyoto 603-8555, Japan*
[4]*Advanced Science Research Center, Japan Atomic Energy Agency, Tokai, Ibaraki 319-1195, Japan*

(Received 6 July 2023; accepted 22 September 2023; published 17 October 2023)

We performed angle-resolved photoemission spectroscopy (ARPES) experiments using soft x rays to investigate the electronic structure of the heavy-fermion superconductor UPt_3. The overall band structure revealed by the present ARPES measurements is compared with density-functional calculations for UPt_3 and the non-$5f$ reference compound $ThPt_3$. We showed that the calculation for $ThPt_3$ gives a better description of the experimental band structure, except for the $5f$-derived heavy quasiparticle bands. This situation is reminiscent of Ce-based heavy-fermion systems, whose band structures are often very similar to those of non-$4f$ La-based compounds. The narrow heavy quasiparticle bands are located just below the Fermi level (E_F), and their band structure could not be resolved by the present energy resolution. We also showed that most of the U $5f$ spectral weight exists not as the coherent heavy-fermion bands but as incoherent components that distribute over a wide energy range, spanning from near E_F to approximately 2 eV. This result indicates that the heavy quasiparticle bands are enormously renormalized by the electron correlation effect. Additionally, we showed that the spectral intensity of the heavy-fermion bands is almost temperature independent, at least up to 100 K, where the magnetic susceptibility follows a Curie-Weiss behavior.

DOI: 10.1103/PhysRevB.108.165127

I. INTRODUCTION

Uranium compounds show a wide variety of intriguing properties such as heavy-fermion state, non-Fermi-liquid behavior, and unconventional superconductivity owing to a complex many-body interaction between localized $5f$ and conduction electrons [1–5]. The ground state of a uranium compound is generally believed to be determined by the hybridization strength between the $5f$ and conduction electrons with respect to the onsite Coulomb interaction. For a weak hybridization limit, a magnetic ground state consisting of localized $5f$ moments would be realized to reduce the onsite Coulomb interaction energy. With increasing hybridization strength, the magnetic ground state is expected to change to a paramagnetic ground state via a quantum critical point (QCP).

Low-temperature properties of uranium compounds are governed by the low-energy excitation spectrum from a complex many-body ground state. It is commonly accepted that the low-energy excitation for a paramagnetic state with large hybridization can be understood by the concept of quasiparticles in the Fermi-liquid theory, whose effective mass becomes heavier with approaching the QCP. The quasiparticle excitation spectrum of the paramagnetic state seems to change at a QCP because of the occurrence of the symmetry breaking in the ground state, and with further decreasing the hybridization, the quasiparticle picture is considered to collapse before reaching the localized limit where U $5f$ electrons are decoupled from the band structure formation. How such a breakdown of quasiparticles arises in real materials and whether it occurs concomitantly with a QCP are subjects of the current debate [6]. The electronic states around QCPs are particularly interesting because most of the above-mentioned intriguing properties of uranium compounds are found in the vicinity of QCPs [1–5], and they may be governed by quasiparticles on the verge of electron localization.

UPt_3 shows a superconducting transition at $T_c = 0.5$ K, and the superconducting state has multiple phases in the magnetic field and temperature plane, revealing the presence of multiple superconducting order parameters [7]. The above superconducting state emerges from a heavy-fermion state that is formed below a few K. The electronic-specific heat coefficient is largely enhanced to be $\gamma \sim 420$ mJ/mol K^2 [8]. The ratio of the γ value and the T^2 coefficient in the resistivity satisfies the Kadowaki-Woods relation as in other heavy-fermion materials [9]. Moreover, the Pauli susceptibility becomes large: $\chi_c \sim 5.0 \times 10^{-3}$ and $\chi_{a,b} \sim 9.0 \times 10^{-3}$ emu/mol for fields along the c axis and in the basal plane, respectively [10]. These results indirectly show that the effective mass of quasiparticles is enormously enhanced, which implies UPt_3 being located in the vicinity of the QCP. The emergence of a long-range antiferromagnetic ordering at extremely low temperatures (below 20 mK) is more convincing evidence of its proximity to the QCP [11]. The presence of heavy quasiparticles is more directly confirmed by the de Haas–van Alphen (dHvA) measurements, and the observed

*kawasaki.ikuto@jaea.go.jp

 ©2023 American Physical Society

effective masses are 10–20 times larger than those in a calculation based on the density-functional theory (DFT) [12].

On the other hand, the magnetic susceptibility deviates from the Pauli-like behavior above about 10 K and exhibits a Curie-Weiss behavior in the high-temperature region above several tens of K [10,13]. The Curie-Weiss behavior is frequently interpreted as evidence for the existence of localized moments, and thus, the quasiparticle picture appears to be broken at high temperatures due to electron localization. Therefore, UPt_3 provides an ideal opportunity to investigate how the strongly renormalized quasiparticles are formed at low temperatures.

The structure of the Fermi surfaces (FSs) of UPt_3 has been intensively studied by means of dHvA measurements [8,14–16]. In the early stages of these studies, the observed dHvA frequencies were interpreted in terms of DFT calculations that assumed $5f$ electrons being itinerant [8,14,15]. Meanwhile, an alternative theoretical model was proposed by Zwicknagl *et al.*, in which two of three $5f$ electrons are localized and do not contribute to the band structure formation [17]. Although the FS shapes of this partially localized model are very different from those of the above itinerant DFT calculations, Zwicknagl *et al.* claimed that their model well explains both the reported dHvA frequencies and the enhancement of quasiparticle mass. Subsequently, McMullan *et al.* carried out detailed dHvA experiments to make a more comprehensive comparison between the experimental FSs and the theoretical FSs of the partially localized model and itinerant DFT calculations. [16]. The dHvA results obtained by McMullan *et al.* lead to a conclusion that the fully itinerant DFT calculation gives a better description of the observed dHvA frequencies.

Despite the experimental FSs being well described by DFT calculations, these calculations cannot reproduce the effective mass of quasiparticles of UPt_3. This means that the bandwidth of heavy quasiparticles is strongly suppressed by the renormalization factor $z_{\boldsymbol{k}} = (1 - \partial \mathrm{Re}\Sigma^R(\boldsymbol{k}, \omega)/\partial\omega)^{-1}$, where $\Sigma^R(\boldsymbol{k}, \omega)$ is the self-energy due to the electron correlation effect. Since $z_{\boldsymbol{k}}$ also suppresses the intensity of heavy quasiparticles in the spectral function, the majority of the $5f$-derived spectral weight would exist as incoherent components rather than as coherent bands.

The spectral function of UPt_3 has been studied by an angle-resolved photoemission spectroscopy (ARPES) experiment with a helium lamp ($h\nu = 21.2$ eV) by Ito *et al.* [18]. In this ARPES study, a very narrow heavy quasiparticle band was observed just below the Fermi level (E_F), and its band structure could not be resolved by the experimental energy resolution (50 meV). They also detected several incoherent satellite spectral features, whose intensities are, however, much smaller than that for the heavy quasiparticle band. Therefore, the vast majority of the U $5f$ spectral weights appear to be not detected in this ARPES study. This is most likely because the U $5f$-derived incoherent components are energetically overlapped with Pt $5d$-derived bands, making it difficult to observe them separately. In this paper, to further investigate the U $5f$ electronic state of UPt_3, we performed ARPES experiments using bulk-sensitive soft x rays [19,20] and experimentally extracted the U $5f$ spectral weights from the photon energy dependence of the photoemission spectra.

II. EXPERIMENTAL DETAILS

We have grown single-crystalline samples of UPt_3 by the Czochralski pulling method. The photoemission experiments were carried out at the soft x-ray undulator beamline BL23SU in SPring-8 [21]. The energy and angular distributions of photoelectrons were measured using a Gammadata-Scienta SES2002 analyzer. The photoemission spectra were measured in the soft x-ray range, i.e., from 495 to 1025 eV. The total energy resolution was set to 70 meV for $h\nu = 495$ and decreased to 180 meV for 1025 eV. The angular resolution along the analyzer slit was $\pm 0.15^\circ$. The binding energy of the photoelectrons was calibrated by the Fermi edge of an evaporated gold film, and the position of ARPES scans in the momentum space was calculated using a free-electron final state model with an inner potential value of $V_0 = 12$ eV [22]. Clean sample surfaces parallel to the (0001) plane were prepared by cleaving *in situ* just before the measurements. The sample temperature was controlled by a liquid helium flow cryostat and maintained at 20 K, except for measurements of temperature dependence. The base pressure of the main chamber was kept better than 9×10^{-9} Pa at 20 K and deteriorated temporarily to around 4×10^{-8} Pa during the measurements of temperature dependence.

III. RESULTS

Figures 1(a) and 1(b) show the ARPES spectra along the Γ-M-Γ′-K-Γ and A-L-A′-H-A lines measured at $h\nu = 495$ and 550 eV, respectively. These photon energies correspond to the k_z values of ∼9 and 9.5 (in units of $2\pi/c$), respectively, and momentum scans in the k_x-k_y plane were done by changing the emission angles of photoelectrons. At these photon energies, the U $5f$ and Pt $5d$ orbitals have dominant contributions because of their strong photoemission cross sections, which are more than one order of magnitude larger than those of other states, such as U $6d$ and Pt $6s$ [23]. In this study, we analyze the ARPES spectra assuming a hexagonal $P6_3/mmc$ structure and ignore the slight trigonal distortion revealed by Walko *et al.* [24]. The integrated area of each energy distribution curve (EDC) normalizes the ARPES spectra. The sample temperature was kept at 20 K, and thus, these ARPES spectra were measured in the paramagnetic phase. Here, the Γ (A) and Γ′ (A′) points represent the same symmetry point, but the former is in the first Brillouin zone (BZ) on the k_x-k_y plane, and the latter is in the second BZ. One can notice that the ARPES spectra differ between the Γ (A) and Γ′(A′) points. This is due to the photoemission structure factor effect, which originates from the interference effect of atomic orbitals with different positions and changes respective band intensities [25]. The crystal structure of UPt_3 consists of two-dimensional U and Pt atomic planes stacked in the c-axis direction, and the difference in the spectra between the Γ (A) and Γ′(A′) points can be ascribed to the change in the interference effect between U and Pt atoms having different positions in the x-y plane. In the vicinity of E_F, there are less dispersive spectral features originating from U $5f$ orbitals both in Figs. 1(a) and 1(b). We will argue the details of these U $5f$-derived spectral weights later in this article. We

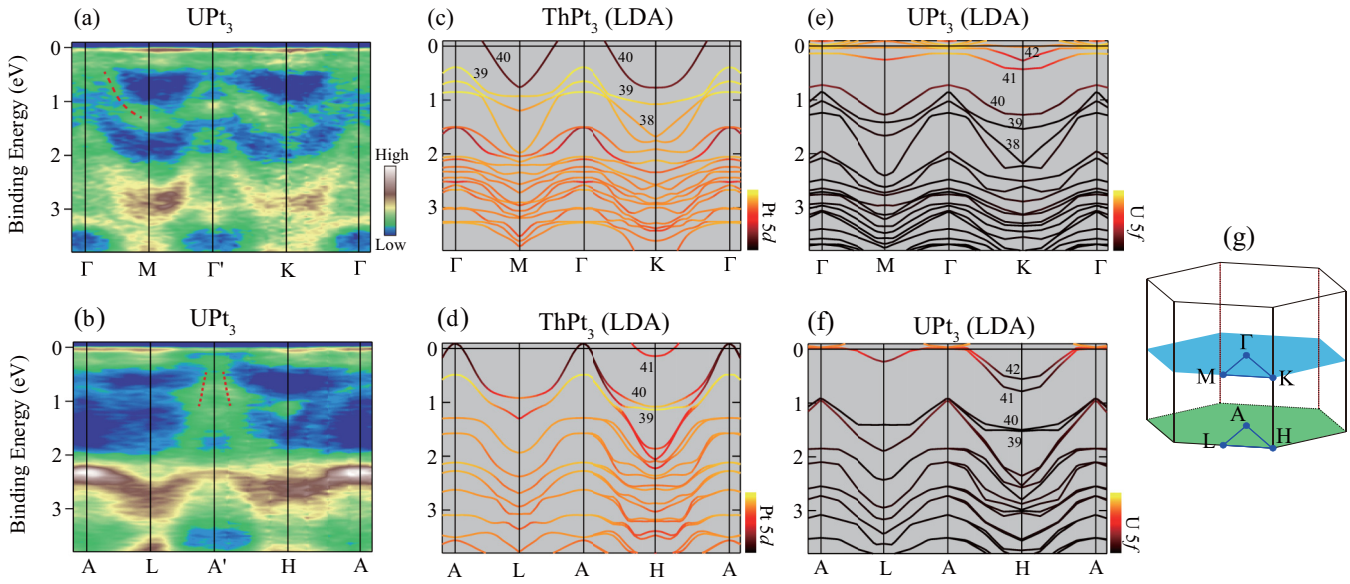

FIG. 1. (a) and (b) ARPES spectra of UPt_3 along the Γ-M-Γ′-K-Γ and A-L-A′-H-A lines measured at $h\nu = 495$ and 550 eV, respectively. The broken red lines are guides to the eyes. (c)–(f) The corresponding calculated band structures for $ThPt_3$ and UPt_3. The color coding of each band represents the contributions of Pt $5d$ or U $5f$ states. (g) Brillouin zone of UPt_3, assuming a hexagonal crystal structure.

also observe several dispersive bands in a whole energy range of Figs. 1(a) and 1(b); these bands are mainly due to the Pt $5d$ orbitals.

For comparison, we carried out band structure calculations for $ThPt_3$ and UPt_3. These calculations are based on a full potential version of a Dirac-type linearized augmented plane wave method within a local density approximation (LDA) [26], and employ experimental lattice constants for UPt_3 [24]. We also assume that $ThPt_3$ has the same crystal structure with UPt_3. The color coding represents the contribution of the Pt $5d$ and U $5f$ components in $ThPt_3$ (LDA) and UPt_3 (LDA). As one can see, both the calculations for $ThPt_3$ and UPt_3 roughly reproduce the non-$5f$ dispersive bands. However, on closer inspection, the calculated bands for $ThPt_3$ seem to give a better agreement for the non-$5f$ experimental bands as follows. As shown in Figs. 1(a) and 1(b), there exist convex spectral features at the Γ and A′ points as indicated by the broken red lines, whose top positions are close to E_F. These spectral features are well reproduced by calculated bands 39 and/or 40 for $ThPt_3$ (LDA), but the peak top positions of bands 39 and 40 for UPt_3 (LDA) are located at deeper binding energies. Calculated bands 39 and 40 for $ThPt_3$ (LDA) have mainly Pt $5d$ and Pt $5p$ orbital characters, the ratio of which varies as a function of momentum, and the same numbered bands of UPt_3 (LDA) have mainly Pt $5d$ character (not shown). It is considered that in UPt_3 (LDA), these bands are pushed toward deeper binding energies because of the interaction with the U $5f$-derives bands 41 and 42. This situation is reminiscent of Ce-based heavy-fermion systems whose band structures are often very similar to those of non-$4f$ La-based compounds, except in the immediate vicinity of E_F [27,28]. The heavy quasiparticle bands for UPt_3 are thus considered to be formed through the hybridization with the dispersive bands, which resemble those for $ThPt_3$.

Next, we investigate the detailed properties of the U $5f$ spectral weights. Figures 2(a) and 2(b) show the ARPES spectra near E_F along the Γ-M-Γ′-K and A-L-A′-H lines measured at $h\nu = 495$ and 550 eV, respectively. In these figures, there exists a less-dispersive narrow peak just below E_F. This is considered to be due to the heavy quasiparticle bands derived from U $5f$ electrons, whose detailed structure cannot be resolved within the energy resolution of the present study. In addition, we observe another peak structure at around 0.25 eV in Figs. 2(a) and 2(b) as indicated by green shaded areas, and its peak position is also found to be almost independent of momentum. We display the calculated band structures for $ThPt_3$ and UPt_3 in Figs. 2(c) to 2(f). Although the calculation for UPt_3 predicts a presence of the weakly dispersive band (band 41) at around 0.25 along the Γ-M-Γ-K line, both calculations predict no flat band at around 0.25 eV for the A-L-A-H line. Therefore, the above peak structure around 0.25 eV appears to be not due to the coherent band component but to an incoherent component caused by the electron correlation effect.

The above-mentioned heavy quasiparticle bands just below E_F and the incoherent component around 0.25 eV are expected to be governed by the U $5f$ spectral weight. In order to confirm this conjecture, we extract the U $5f$ spectral weight from the APRES spectra by utilizing photo energy dependence on the photoemission cross section. In the soft x-ray range, the relative PES cross-section ratio $\sigma_{U5f}/\sigma_{Pt5d}$ decreases with increasing photon energy [23], and therefore, we can extract the U $5f$ component by comparing the EDCs measured at different photon energies. Figures 3(a) to 3(d) show EDCs at the high-symmetry points measured at two different energies, and these EDCs are normalized by the integrated intensity in the region deeper than 2.2 eV, where the Pt $5d$ components dominate the spectra. The spectra measured with lower photon energies are convoluted with a Gaussian function to compensate for differences in the energy resolution, obscuring the peak structure of the incoherent component

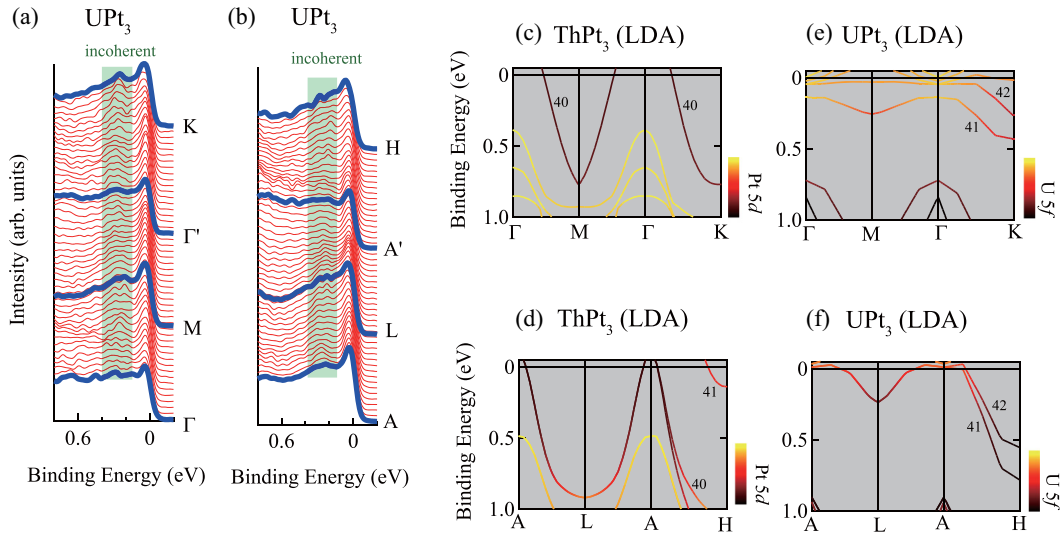

FIG. 2. (a) and (b) ARPES spectra of UPt_3 in the vicinity of E_F along the Γ-M-Γ′-K and A-L-A′-H lines measured at $h\nu = 495$ and 550 eV, respectively. The green shaded areas indicate the positions of incoherent spectral intensities. (c)–(f) The calculated band structures for $ThPt_3$ and UPt_3.

peak at 0.25 eV. Here, $\sigma_{U5f}/\sigma_{Pt5d}$ is estimated to be 1.06, 0.91, and 0.77 for $h\nu = 495$, 805, and 1025 eV, respectively. In Figs. 3(a) to 3(d), we also display the difference spectra, which reflect the U $5f$ spectral weight. These difference spectra show that most of the U $5f$ spectral weight exists not as heavy quasiparticle components but as incoherent components that distribute not only in the vicinity of 0.25 eV but also over the wide binding energy range up to ∼2 eV. We found that these difference spectra show a peak structure at around 1.3 to 1.7 eV except for the H-point, as indicated by arrows; we will discuss the physical interpretation of this peak later in this article. For comparison, we show the calculated U $5f$ partial density of states in Fig. 3(e), which is broadened with the experimental energy resolution for 1025 eV. We can see that the calculation cannot reproduce both the peak structure at around 1.3 to 1.7 eV and the observed U $5f$ spectral as the calculated U $5f$ spectral weight is concentrated in a narrower energy region below E_F. We display the difference spectra along the K-Γ-K-M lines in Fig. 3(e), which reveal that the U $5f$-derived spectral weight forms some structure in this high-symmetry line and thus is not totally independent of momentum.

In the following, we investigate how the ARPES spectra evolve as a function of temperature. Figure 4(a) shows the ARPES spectra along the L-A-L line measured at 10 K and 100 K, respectively, and in Figs. 4(b) and 4(c), the EDCs at the A and L points are selectively displayed. Note that around 100 K, the U $5f$ electrons are considered to have a localized character as the magnetic susceptibility follows a Curie-Weiss behavior [13]. As can be seen in these figures, there seems to be no noticeable temperature dependence except for the slight suppression of the peak-top intensity of heavy quasiparticle bands at E_F. In order to evaluate the temperature dependence of the total intensity of the heavy quasiparticle bands, we have integrated the spectra in Figs. 4(b) and 4(c) over 0.15 to −0.2 eV range, which is indicated by the green shaded region in the inset of Fig. 4(b). We confirmed that the integrated intensities for the A and L points hardly depend on temperature and decrease by only 3% at most with increasing temperature from 10 K to 100 K.

IV. DISCUSSION

In this paper, we have performed ARPES experiments to investigate the U $5f$ electronic state in UPt_3. We have revealed that the U $5f$ spectral weight distributes over a wide binding energy range from E_F to ∼2 eV, most of which exists as incoherent components. Here, we discuss the physical implications of these results. It is generally believed that the competition between the Kondo effect and the RKKY interaction determines the ground state of f-electron systems; both of them evolve as a function of $|J_{cf}|D(\epsilon_F)$ [29]. Here, $D(\epsilon_F)$ and $|J_{cf}|$ represent the density of states at E_F and the magnetic coupling strength between conduction and f electrons, respectively. This situation can be summarized in the so-called Doniach phase diagram [Fig. 5(a)]. Given that UPt_3 does not host well-defined long-range magnetic order and exhibits a heavy-fermion behavior, it is considered to be located on the right-hand side of the QCP in the Doniach phase diagram. Strictly speaking, the development of an antiferromagnetic order at the extremely low temperature of 20 mK has been confirmed [11], but we ignore this magnetic ordering in this discussion because of the smallness of its energy scale.

The f-electron spectral function at zero temperature is defined as

$$\rho^f(\boldsymbol{k}, \omega) = -\frac{1}{\pi}\mathrm{Im}G_f^R(\boldsymbol{k}, \omega). \quad (1)$$

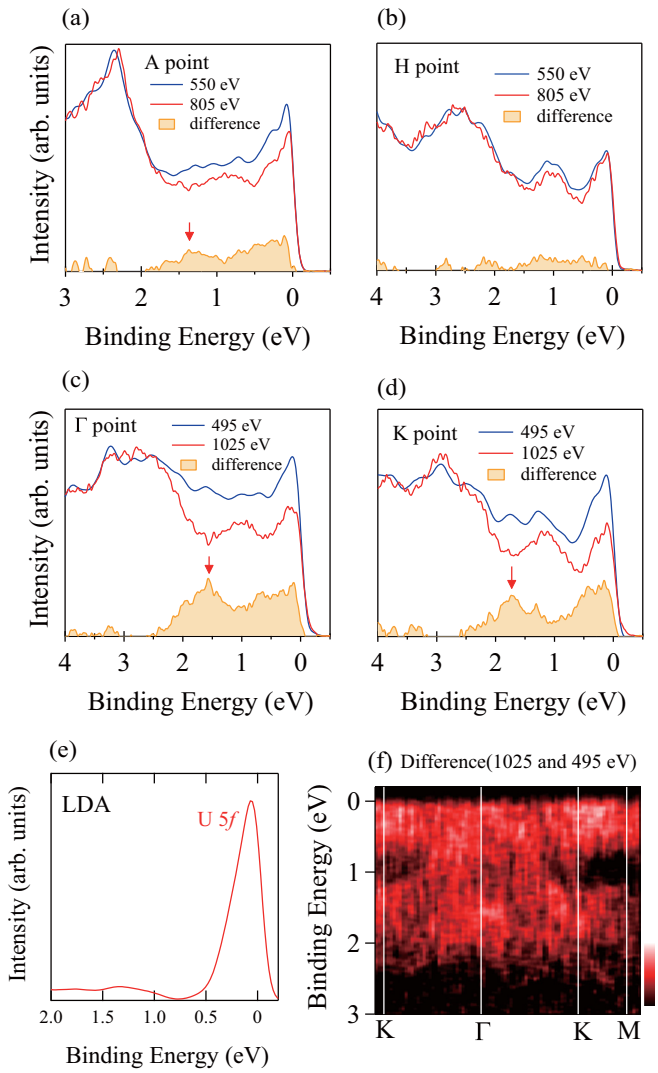

FIG. 3. (a)–(d) ARPES spectra of UPt_3 at the high-symmetry points measured at two different photon energies. The spectra measured with lower photon energies are convoluted with a Gaussian function to compensate for the differences in the energy resolutions. These spectra are normalized by the integrated intensity below 2.2 eV, where the spectral intensities are dominated by the Pt 5*d* components. The difference curves, which are considered to reflect U 5*f* spectral weight, are also shown. (e) Calculated U 5*f* partial density of states. (f) Difference spectra along the high-symmetry lines between the spectra taken at different photon energies.

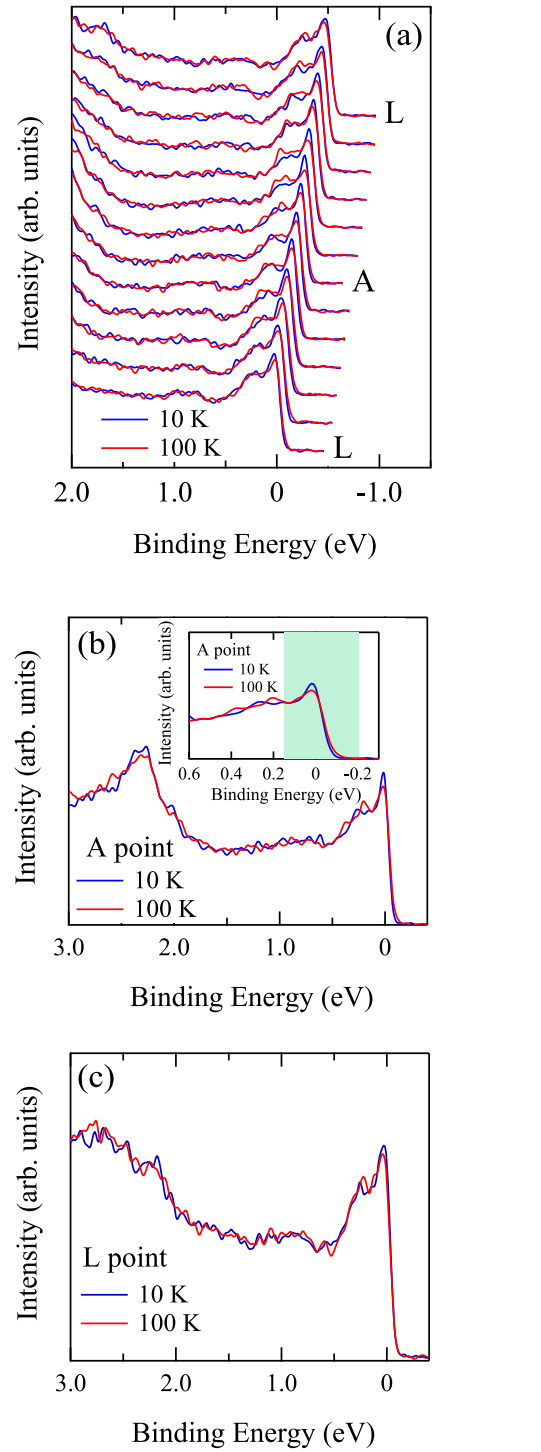

FIG. 4. (a) Comparison of ARPES spectra along the L-A-L line measured at 10 and 100 K, respectively. The spectra are shown with offsets for better viewing. (b) and (c) Temperature variations of the ARPES spectra at the high-symmetry points. The inset shows an enlarged view of the area E_F region.

The retarded Green function for f electrons $G_f^R(\boldsymbol{k}, \omega)$ can be expressed in the following form:

$$G_f^R(\boldsymbol{k}, \omega) = \frac{1}{N_m} \sum_m \left\langle \Phi_0^N \middle| f_{\boldsymbol{k}m} \frac{1}{\hbar\omega + E_0 - \hat{H} + i\eta} f_{\boldsymbol{k}m}^\dagger \middle| \Phi_0^N \right\rangle + \frac{1}{N_m} \sum_m \left\langle \Phi_0^N \middle| f_{\boldsymbol{k}m}^\dagger \frac{1}{\hbar\omega - E_0 + \hat{H} + i\eta} f_{\boldsymbol{k}m} \middle| \Phi_0^N \right\rangle, \tag{2}$$

where $|\Phi_0^N\rangle$ and E_0 stand for the ground state of the total system and the ground-state energy, respectively. $f_{\boldsymbol{k}m}^\dagger$ is a creation operator for f electrons having a wave vector $\boldsymbol{k}$. m is the quantum number for the spin and orbital freedom, and N_m represents the Hilbert space dimension for m. η is introduced as an infinitely small positive broadening parameter. The first and second terms in Eq. (2)

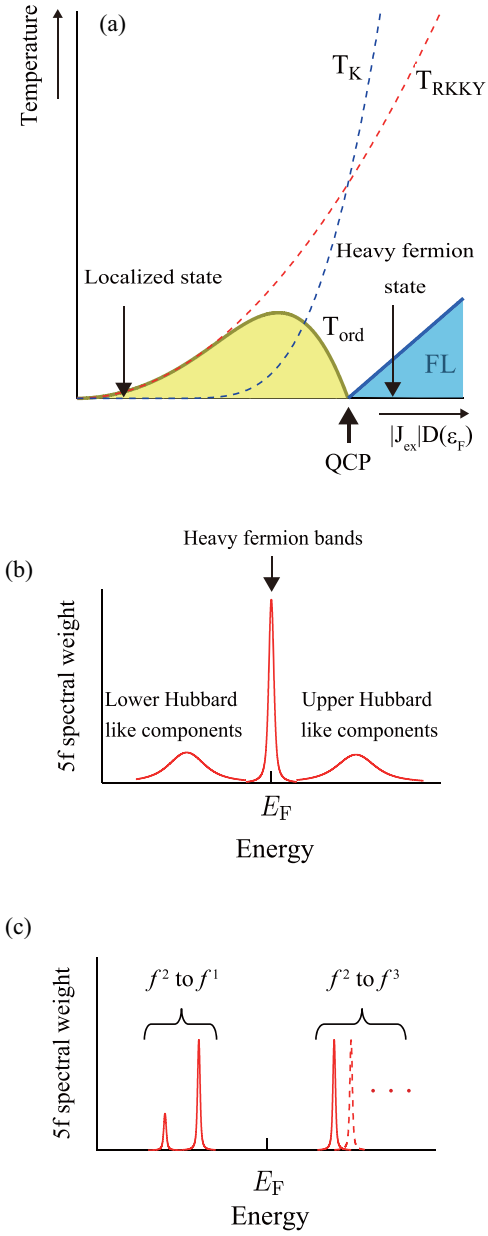

FIG. 5. (a) Doniach phase diagram. FL denotes the Fermi-liquid state. (b) and (c) Schematic illustrations of the $5f$ spectral functions in the heavy-fermion state and localized limit, respectively.

correspond to inverse photoemission and photoemission processes. Here, a negative $\hbar\omega$ value corresponds to a positive binding energy.

The above spectral and Green functions are defined assuming zero temperature, but they can be extended to finite temperatures by employing the grand-canonical ensemble average [30]. The f-electron spectral function at finite temperatures is described as

$$\begin{aligned}\rho^f(\boldsymbol{k},\omega,T) &= \rho^f_{\mathrm{BIS}}(\boldsymbol{k},\omega,T) + \rho^f_{\mathrm{PES}}(\boldsymbol{k},\omega,T),\\ \rho^f_{\mathrm{BIS}}(\boldsymbol{k},\omega,T) &= \frac{1}{1+e^{-\beta\hbar\omega}}\rho^f(\boldsymbol{k},\omega,T),\\ \rho^f_{\mathrm{PES}}(\boldsymbol{k},\omega,T) &= \frac{1}{1+e^{\beta\hbar\omega}}\rho^f(\boldsymbol{k},\omega,T),\end{aligned} \tag{3}$$

where $\rho^f_{\mathrm{BIS}}(\boldsymbol{k},\omega,T)$ and $\rho^f_{\mathrm{PES}}(\boldsymbol{k},\omega,T)$ are inverse photoemission and photoemission components in the finite-temperature spectral function. β represents $1/k_{\mathrm{B}}T$, and k_{B} is the Boltzmann constant. The prefactors $(1+e^{-\beta\hbar\omega})^{-1}$ and $(1+e^{\beta\hbar\omega})^{-1}$ serve to extract ρ_{BIS} and ρ_{PES} from the finite-temperature spectral function. The detailed functional form of $\rho^f(\boldsymbol{k},\omega,T)$ is described in Ref. [30].

Despite the exact solution for the f-electron spectral function being not available, it is generally considered that in the heavy-fermion region, i.e., on the right-hand side of the QCP in Fig. 5(a), the f-electron spectral function at low temperatures has a three-peak structure as shown schematically in Fig. 5(b). The peak located around E_{F} corresponds to excitations of heavy quasiparticles. Here, we ignore the detailed band structure of the heavy quasiparticle bands. The spectral intensity and width of the heavy quasiparticle band are suppressed by the renormalization factor $z_{\boldsymbol{k}} = (1 - \partial\mathrm{Re}\Sigma^R(\boldsymbol{k},\omega)/\partial\omega)^{-1}$. Since the total intensity of the spectral function at each $\boldsymbol{k}$ point is always conserved, the incoherent components, which are located away from E_{F}, develop under the presence of the electron correlation effect [30]. These incoherent components correspond to the lower and upper Hubbard bands in the Hubbard model. These Hubbard-like bands may consist of more than one component for a multi-f-electron system, but such fine structures are ignored in this figure. The above-mentioned basic structure of the spectral function in the heavy-fermion region is directly applicable for UPt_3.

On the other hand, in the localized limit, where the hybridization between f and conduction electrons vanishes, the properties of the f-electron spectral function are well known. In this localized limit, the integer valence state should be realized, and the f-electron spectral function should be dominated by localized excitations, as schematically shown in Fig. 5(c). In Fig. 5(c), the f^2 ground state is assumed, and there exist two multiplets that correspond to excitations from f^2 to f^1 states and from f^2 to f^3 states. See Refs. [31–34] for the detailed structure of these localized excitations. These spectral weights of localized excitations are independent of momentum and temperature as long as $k_{\mathrm{B}}T$ is much smaller than the energy scale of the binding energy of the bare $5f$ electrons and the onsite Coulomb interaction. In fact, ARPES experiments for the localized $5f^2$ system UPd_3 have revealed that the $5f$-electron spectral function is dominated by less-dispersive f^2 to f^1 excitations: the ${}^2F_{5/2}$ and ${}^2F_{7/2}$ final state components [35]. The energy separation of these final-state components is about 0.8 eV, and this value has been roughly reproduced by a calculation for an isolated atomic configuration [34].

In this study, we have derived the U $5f$ spectral weight from the $h\nu$ dependence of the ARPES spectra, as shown in Figs. 3(a) to 3(d), and have shown that most of the U $5f$ spectral weight exists as incoherent components. This result means that the heavy quasiparticle bands are strongly renormalized, i.e., the renormalization factor $z_{\boldsymbol{k}}$ for these bands is markedly reduced from unity. This situation is consistent with the dHvA and specific heat measurements, both of which have shown the effective electron masses being highly enhanced in UPt_3 [8,12]. We also have revealed that the incoherent components distribute not only in the vicinity of the peak at 0.25 eV but

also over a wide binding energy range up to ∼2 eV and exhibit another peak structure at around 1.3∼1.7 eV for several high-symmetry points. Note that the energy separation between 0.25 and 1.3∼1.7 eV peaks is 1∼1.45 eV, which is comparable to the above-mentioned energy separation between the $^2F_{5/2}$ and $^2F_{7/2}$ final state peaks for UPd_3, indicating that the incoherent components for UPt_3 can possibly be viewed as a precursor of f^2 to f^1 multiplet in the localized limit. However, as shown in Fig. 3(f), the incoherent components are not totally independent of momentum. Therefore, the observed spectral shape of the incoherent components in the energy and momentum space is considered to reflect an intermediate electronic state between the itinerant and localized limits.

Finally, we would like to discuss the physical implication of the almost absence of temperature dependence of the ARPES spectra. As shown in Figs. 4(a) to 4(c), the temperature dependence of the spectra is not observed except for the slight suppression of the peak-top intensities of heavy quasiparticle bands in the temperature range 10–100 K. First, we would like to discuss the electronic state at the lower temperature side (10 K). According to the specific heat and resistivity measurements, to observe the well-defined Fermi-liquid-like temperature dependence, low temperatures below 1.5 K are required [7]. Therefore, some deviation from the Fermi-liquid behavior exists already at 10 K, although the resistivity starts to drop rapidly, and the magnetic susceptibility hardly depends on temperature below 10 K [7,10]. Therefore, the lifetime of the heavy quasiparticles is not long enough compared to k_BT at 10 K. However, such a lifetime broadening seems negligible in the present ARPES experiments below 20 K as follows. If we assume the lifetime broadening of excited quasiparticles is comparable to $1.5k_BT$ at 1.5 K, the lifetime broadening is expected to increase to be approximately $67k_BT$ at 10 K as the lifetime broadening is proportional to T^2 according to the Fermi-liquid theory [36]. Nevertheless, this value of $67k_BT$ is negligibly small compared to the present energy resolution of 70∼180 meV, an order of 1 000 k_BT. The same argument can be applied at the temperature of 20 K, where most of the ARPES spectra of the present study were taken since the lifetime broadening value at 20 K ($\sim 267k_BT$) is still smaller than the present energy resolution. These arguments support that the lifetime broadening effect for thermally excited quasiparticles is unlikely to be seen below 20 K at the current energy resolution.

Next, we would like to discuss the electronic state at the higher temperature side of 100 K. As noted in the Introduction, the magnetic susceptibility for UPt_3 follows a Curie-Weiss law in the high-temperature region above several tens of K [13], and the Curie-Weiss behavior is often considered as evidence for the existence of local f moments. If the $5f$ electrons are totally localized at 100 K, the U $5f$ spectral function should change to that in the localized limit [Fig. 5(c)]. However, as our study shows, the ARPES spectra at 100 K are almost identical to those at 10 K except for the slight suppression of the peak-top intensity of heavy quasiparticle bands at E_F, and the integrated intensities of the heavy quasiparticle bands decrease only 3% at most with increasing temperature from 10 to 100 K. The almost absence of the temperature dependence of the integrated intensities implies that the slight suppression of heavy quasiparticle band intensity can be naturally explained without contradiction by the prefactor $(1 + e^{\beta\hbar\omega})^{-1}$ in Eq. (3) whose functional form is equivalent to the Fermi-Dirac function and that the spectral function $\rho^f(\boldsymbol{k}, \omega, T)$ depends hardly on temperature. This leads us to conclude that the renormalization factor $z_{\boldsymbol{k}}$ for heavy quasiparticles is almost independent of temperature in the temperature range of the present study. Based on these arguments, we suggest that the Curie-Weiss behavior in UPt_3 should not be understood in terms of a simple ensemble of localized $5f$ moments but rather in terms of a quasiparticle picture with a shorter lifetime owing to thermal excitations.

The observed weak dependence of the heavy quasiparticle intensity on temperature for UPt_3 is in stark contrast to ARPES experiments for USb_2 [37]. In this ARPES study, the intensity of narrow $5f$ bands just below E_F is suppressed monotonously with increasing temperature and almost disappears at 130 K, indicative of a dramatic change in $\rho^f(\boldsymbol{k}, \omega, T)$ as a function of temperature. Similar behavior has been reported for $4d$-$4f$ resonant ARPES experiments performed for the Ce-based heavy-fermion compounds whose intensity of the heavy-fermion bands monotonously decreases with increasing temperature [38–42]. At present, the origin of the difference between USb_2 and UPt_3 remains unknown. The temperature dependence of FSs of the Yb-based heavy fermion compound $YbRh_2Si_2$ has been studied by ARPES and Compton-scattering experiments [43,44]; the former experiment revealed that the FSs do not change their sizes or shape up to around 100 K, well above the Kondo temperature (∼25 K), while the latter experiment claims that a FS reconstruction occurs at room temperature due to the localization of $4f$ electrons. Direct comparison of these studies with our UPt_3 result is difficult as we could not resolve the FS structure, but our ARPES result agrees with the ARPES result for $YbRh_2Si_2$ regarding the absence of the temperature dependence.

V. CONCLUSION

We investigated the electronic structure of the heavy-fermion superconductor UPt_3 by soft x-ray photoemission spectroscopy. The ARPES results were compared with the band structure calculations for UPt_3 and the non-$5f$ reference compound $ThPt_3$. The observed band structure, except for the heavy quasiparticle bands at E_F, is well described by the calculation for $ThPt_3$ rather than that for UPt_3. The heavy quasiparticle bands seem to be formed through the hybridization between dispersive bands, which resemble those for $ThPt_3$, and the U $5f$ components near E_F. We extracted the U $5f$ spectral weight from the photon energy dependence of the ARPES spectra and have shown that most of the U $5f$ spectral weight exists not as the coherent heavy-fermion bands but as incoherent components which distribute over a wide energy range from near E_F to ∼2 eV. The incoherent components exhibit peaks at 0.25 and 1.3∼1.7 eV at several high-symmetry points, and the energy separation of these peaks is comparable to that of the f^1 final-state peaks observed in the f^2 localized compound UPd_3, indicating that the incoherent component for UPt_3 can possibly

be viewed as a precursor of f^2 to f^1 multiplet for the localized limit. The spectral intensity of the coherent heavy quasiparticle bands hardly depends on temperature, at least up to 100 K, where the magnetic susceptibility follows a Curie-Weiss law.

ACKNOWLEDGMENTS

This work was performed under Proposals No. 2021A3811 and No. 2021B3811 at SPring-8 BL23SU and was financially supported by JSPS KAKENHI Grant No. 22J03871.

[1] G. R. Stewart, Rev. Mod. Phys. **73**, 797 (2001).
[2] G. R. Stewart, Rev. Mod. Phys. **78**, 743 (2006).
[3] C. Pfleiderer, Rev. Mod. Phys. **81**, 1551 (2009).
[4] O. Stockert, S. Kirchner, F. Steglich, and Q. Si, J. Phys. Soc. Jpn. **81**, 011001 (2012).
[5] B. White, J. Thompson, and M. Maple, Physica C **514**, 246 (2015).
[6] M. Vojta, J. Low Temp. Phys. **161**, 203 (2010).
[7] R. Joynt and L. Taillefer, Rev. Mod. Phys. **74**, 235 (2002).
[8] N. Kimura, R. Settai, Y. Ōnuki, H. Toshima, E. Yamamoto, K. Maezawa, H. Aoki, and H. Harima, J. Phys. Soc. Jpn. **64**, 3881 (1995).
[9] K. Kadowaki and S. Woods, Solid State Commun. **58**, 507 (1986).
[10] A. Galatanu, Y. Haga, T. D. Matsuda, S. Ikeda, E. Yamamoto, D. Aoki, T. Takeuchi, and Y. Ōnuki, J. Phys. Soc. Jpn. **74**, 1582 (2005).
[11] Y. Koike, N. Metoki, N. Kimura, E. Yamamoto, Y. Haga, Y. Ōnuki, and K. Maezawa, J. Phys. Soc. Jpn. **67**, 1142 (1998).
[12] N. Kimura, T. Tani, H. Aoki, T. Komatsubara, S. Uji, D. Aoki, Y. Inada, Y. Ōnuki, Y. Haga, E. Yamamoto, and H. Harima, Physica B **281-282**, 710 (2000).
[13] A. De Visser, A. Menovsky, and J. Franse, Physica B+C **147**, 81 (1987).
[14] L. Taillefer, R. Newbury, G. Lonzarich, Z. Fisk, and J. Smith, J. Magn. Magn. Mater. **63-64**, 372 (1987).
[15] L. Taillefer and G. G. Lonzarich, Phys. Rev. Lett. **60**, 1570 (1988).
[16] G. J. McMullan, P. M. C. Rourke, M. R. Norman, A. D. Huxley, N. Doiron-Leyraud, J. Flouquet, G. G. Lonzarich, A. McCollam, and S. R. Julian, New J. Phys. **10**, 053029 (2008).
[17] G. Zwicknagl, A. N. Yaresko, and P. Fulde, Phys. Rev. B **65**, 081103(R) (2002).
[18] T. Ito, H. Kumigashira, H.-D. Kim, T. Takahashi, N. Kimura, Y. Haga, E. Yamamoto, Y. Ōnuki, and H. Harima, Phys. Rev. B **59**, 8923 (1999).
[19] A. Sekiyama, T. Iwasaki, K. Matsuda, Y. Saitoh, Y. Ōnuki, and S. Suga, Nature (London) **403**, 396 (2000).
[20] S. Tanuma, C. J. Powell, and D. R. Penn, Surf. Interface Anal. **43**, 689 (2011).
[21] Y. Saitoh, Y. Fukuda, Y. Takeda, H. Yamagami, S. Takahashi, Y. Asano, T. Hara, K. Shirasawa, M. Takeuchi, T. Tanaka, and H. Kitamura, J. Synchrotron Radiat. **19**, 388 (2012).
[22] S.-i. Fujimori, M. Kobata, Y. Takeda, T. Okane, Y. Saitoh, A. Fujimori, H. Yamagami, Y. Matsumoto, E. Yamamoto, N. Tateiwa, and Y. Haga, Phys. Rev. B **96**, 125117 (2017).
[23] J. Yeh and I. Lindau, At. Data Nucl. Data Tables **32**, 1 (1985).
[24] D. A. Walko, J.-I. Hong, T. V. Chandrasekhar Rao, Z. Wawrzak, D. N. Seidman, W. P. Halperin, and M. J. Bedzyk, Phys. Rev. B **63**, 054522 (2001).
[25] H. Daimon, S. Imada, H. Nishimoto, and S. Suga, J. Electron Spectrosc. Relat. Phenom. **76**, 487 (1995).
[26] H. Yamagami, J. Phys. Soc. Jpn. **67**, 3176 (1998).
[27] Q. Y. Chen, X. B. Luo, E. Vescovo, K. Kaznatcheev, F. J. Walker, C. H. Ahn, Z. F. Ding, Z. H. Zhu, L. Shu, Y. B. Huang, and J. Jiang, Phys. Rev. B **100**, 035117 (2019).
[28] Y. Saitoh, H. Fujiwara, T. Yamaguchi, Y. Nakatani, T. Mori, H. Fuchimoto, T. Kiss, A. Yasui, J. Miyawaki, S. Imada, H. Yamagami, T. Ebihara, and A. Sekiyama, J. Phys. Soc. Jpn. **85**, 114713 (2016).
[29] S. Doniach, Physica B+C **91**, 231 (1977).
[30] A. L. Fetter and J. D. Walecka, *Quantum Theory of Many Particle Systems* (Dover, New York, 2003).
[31] Y. Baer and J. Schoenes, Solid State Commun. **33**, 885 (1980).
[32] V. Kaufman and L. J. Radziemski, J. Opt. Soc. Am. **66**, 599 (1976).
[33] N. Beatham, P. Cox, A. Orchard, and I. Grant, Chem. Phys. Lett. **63**, 69 (1979).
[34] C. Danilo, V. Vallet, J.-P. Flament, and U. Wahlgren, J. Chem. Phys. **128**, 154310 (2008).
[35] I. Kawasaki, S.-i. Fujimori, Y. Takeda, T. Okane, A. Yasui, Y. Saitoh, H. Yamagami, Y. Haga, E. Yamamoto, and Y. Ōnuki, Phys. Rev. B **87**, 075142 (2013).
[36] K. Yamada, *Electron Correlation in Metals* (Cambridge University Press, Cambridge, England, 2004).
[37] Q. Y. Chen, X. B. Luo, D. H. Xie, M. L. Li, X. Y. Ji, R. Zhou, Y. B. Huang, W. Zhang, W. Feng, Y. Zhang, L. Huang, Q. Q. Hao, Q. Liu, X. G. Zhu, Y. Liu, P. Zhang, X. C. Lai, Q. Si, and S. Y. Tan, Phys. Rev. Lett. **123**, 106402 (2019).
[38] Q. Y. Chen, D. F. Xu, X. H. Niu, J. Jiang, R. Peng, H. C. Xu, C. H. P. Wen, Z. F. Ding, K. Huang, L. Shu, Y. J. Zhang, H. Lee, V. N. Strocov, M. Shi, F. Bisti, T. Schmitt, Y. B. Huang, P. Dudin, X. C. Lai, S. Kirchner *et al.*, Phys. Rev. B **96**, 045107 (2017).
[39] Q. Y. Chen, D. F. Xu, X. H. Niu, R. Peng, H. C. Xu, C. H. P. Wen, X. Liu, L. Shu, S. Y. Tan, X. C. Lai, Y. J. Zhang, H. Lee, V. N. Strocov, F. Bisti, P. Dudin, J.-X. Zhu, H. Q. Yuan, S. Kirchner, and D. L. Feng, Phys. Rev. Lett. **120**, 066403 (2018).
[40] Q. Y. Chen, C. H. P. Wen, Q. Yao, K. Huang, Z. F. Ding, L. Shu, X. H. Niu, Y. Zhang, X. C. Lai, Y. B. Huang, G. B. Zhang, S. Kirchner, and D. L. Feng, Phys. Rev. B **97**, 075149 (2018).
[41] Q. Yao, D. Kaczorowski, P. Swatek, D. Gnida, C. H. P. Wen, X. H. Niu, R. Peng, H. C. Xu, P. Dudin, S. Kirchner, Q. Y. Chen, D. W. Shen, and D. L. Feng, Phys. Rev. B **99**, 081107(R) (2019).

[42] Y. Wu, Y. Zhang, F. Du, B. Shen, H. Zheng, Y. Fang, M. Smidman, C. Cao, F. Steglich, H. Yuan, J. D. Denlinger, and Y. Liu, Phys. Rev. Lett. **126**, 216406 (2021).

[43] K. Kummer, S. Patil, A. Chikina, M. Güttler, M. Höppner, A. Generalov, S. Danzenbächer, S. Seiro, A. Hannaske, C. Krellner, Y. Kucherenko, M. Shi, M. Radovic, E. Rienks, G. Zwicknagl, K. Matho, J. W. Allen, C. Laubschat, C. Geibel, and D. V. Vyalikh, Phys. Rev. X **5**, 011028 (2015).

[44] M. Güttler, K. Kummer, K. Kliemt, C. Krellner, S. Seiro, C. Geibel, C. Laubschat, Y. Kubo, Y. Sakurai, D. V. Vyalikh, and A. Koizumi, Phys. Rev. B **103**, 115126 (2021).